Tissue Oxygen Depth Explorer (TODE): An Interactive Database for Microscopic Oxygen Imaging Data

Layth N. Amra[1], Philipp Mächler[2], Natalie Fomin-Thunemann[1], Kıvılcım Kılıç[1], Payam Saisan[3], Anna Devor[1,4], Martin Thunemann[1,*]

[1]Department of Biomedical Engineering, Boston University, Boston, MA 02215, USA.

[2]Department of Physics, University of California, San Diego, La Jolla, CA 92093, USA.

[3]Department of Radiology, University of California, San Diego, La Jolla, CA,92093, USA.

[4]Martinos Center for Biomedical Imaging, MGH, Harvard Medical School, Charlestown, MA 02129, USA.

Key words: Two-photon, phosphorescence, lifetime, metabolism, CMRO2

Correspondence:

Dr. Martin Thunemann

Boston University

610 Commonwealth Avenue

Boston, MA, 02115, USA

Email: martinth@bu.edu

Phone: +1 657 244 3541

Introduction

Over the last decade, increased efforts were made to standardize curation, storage, and retrieval of scholar data (Data Citation Synthesis Group 2014, Nosek, Alter et al. 2015, Wilkinson, Dumontier et al. 2016), even such heterogenous as generated in experimental neurosciences (Rubel, Tritt et al. 2022). Public availability of experimental data ensures independent validation of published studies beyond the peer-review process. Equally important, it facilitates secondary use of experimental data, for example, to generate or validate computational models without needing to reperform complex in vivo experiments. In this context, the FAIR guidelines ensure standards where data is Findable, Accessible, Interoperable, and Reusable (Wilkinson, Dumontier et al. 2016). Scientific journals and funding agencies encourage - or enforce - data sharing within the scientific community by requesting researchers to make their data publicly available (Kim, Kim et al. 2020, NIH 2020, NSF 2021, Science Magazine 2023, SpringerNature 2023) and by defining reporting requirements for commonly used data modalities. However, less frequently used experimental modalities typically lack well-defined data standards, so researchers rely on individual solutions to provide data in a form that is accessible, understandable, and reusable by other researchers. Such a case is two-photon-based phosphorescence lifetime microscopy (2P-PLM) used for quantitative oxygen measurements in live animals (Sakadzic, Roussakis et al. 2010, Lecoq, Parpaleix et al. 2011) - a technique that is used by a small but growing community of researchers. Although based on standard two-photon laser scanning microscopy platforms, 2P-PLM generates data that is more complex and does not fall into the scope of databases dedicated to standard microscopic imaging experiments.

Given these limitations, we developed the MATLAB-based “Tissue Oxygen Depth Explorer (TODE) v1.0”, a MATLAB-based database with graphical user interface (GUI) to simplify access and visualization of raw and pre-processed 2P-PLM oxygen imaging data. The datasets

included with TODE v1.0 were generated as part of our recent 2P-PLM-based study on oxygen metabolism across cortical layers in awake mice under ‘resting-state’ conditions (Mächler, Fomin-Thunemann et al. 2022).

The cerebral metabolic rate of oxygen ($CMRO_2$) is mostly dictated by metabolic demands of neuronal activity and a central parameter for the general understanding of brain energetics as well as the interpretation of blood oxygenation level–dependent magnetic resonance imaging (Heeger and Ress 2002). From histological studies, it has been predicted that $CMRO_2$ is higher in cortical layer IV than layer I (Gonzalez-Lima and Cada 1994, Weber, Keller et al. 2008). To address this prediction in vivo, we used 2P-PLM to measure tissue oxygen levels around penetrating arterioles at different cortical depths in awake mice under ‘resting-state’ conditions (Mächler, Fomin-Thunemann et al. 2022). Penetrating arterioles traverse the cerebral cortex from the surface towards the white matter and branch at variable depths to form a dense capillary network (Blinder, Tsai et al. 2013). The exception is an area around penetrating arterioles largely devoid of capillaries resulting in prominent gradients from high pO_2 close to the arteriole to low pO_2 within the tissue. We had previously adapted the assumptions of the Krogh model to better represent this vessel geometry allowing to estimate $CMRO_2$ at different cortical depths based on these pO_2 gradients (Mächler, Fomin-Thunemann et al. 2022). In contrast to previous predictions, we observed the highest $CMRO_2$ in layer I and not in layer IV.

In the current paper, we present the MATLAB-based TODE database and GUI for easy access to the primary data generated in our recent study (Mächler, Fomin-Thunemann et al. 2022). This application allows us to share these datasets in a form that facilitates close inspection by the research community and their use for alternative modeling approaches of cortical oxygen diffusion and metabolism.

Methods

Data collection and analysis

For animal preparation and further experimental details on data acquisition, see (Mächler, Fomin-Thunemann et al. 2022). All experiments were approved by the animal care and use committees at UC San Diego and Boston University. Two-photon microscopy was performed on a commercial two-photon setup (Bruker) with femtosecond Ti:Sapphire laser (Coherent). The two-photon excitable phosphorescent dye Oxyphor 2P (Esipova, Barrett et al. 2019) was provided by S. Vinogradov (University of Pennsylvania); a solution of Oxyphor 2P in artificial cerebral spinal fluid was pressure-microinjected through a silicone port (Roome and Kuhn 2014) into the barrel cortex of awake mice. We added Sulforhodamine 101 labeling astrocytes to control potential tissue damage due to the injection procedure. Vascular stacks were acquired at low (4× and 5× objective) and high (20× objective at 1× and 2× zoom) magnification after intravenous injection of commercially available fluorescein isothiocyanate (FITC)-labeled dextran or custom-conjugated Alexa 680-Dextran (Li, Ohtomo et al. 2019). We performed 2P-PLM measurements at one or two penetrating arterioles in 1-2 sessions per animal at 0-500 µm below the cortical surface. Oxyphor 2P was excited at a wavelength of 950 nm at 400 individual points per depth plane that were oriented in radial or square grids around the penetrating arteriole. Oxyphor 2P phosphorescence was collected with a photon-counting Gallium Arsenide photomultiplier tube (Hamamatsu). During data collection, acquisition runs were divided into 20 iterations, in each of which 50 individual excitation-decay cycles of all 400 points were acquired. Data was then transferred for post-processing into MATLAB (2019-2023). Some iterations were excluded if animal motion measured with an accelerometer exceeded a custom-set threshold during acquisition of these iterations. The final phosphorescence decay profile was estimated from the sum of 500-1000 acquisition cycles per point – depending on the number of excluded iterations. Non-linear least squares fitting (using the MATLAB function “lsqnonlin”) of a single

exponential decay function was performed to estimate the decay time constant τ. Then, we used the Stern-Volmer equation to estimate pO_2 (in mmHg) from τ using in-vitro calibration parameters measured for the respective Oxyphor 2P batches (Esipova, Barrett et al. 2019). To normalize photon counts across measurements, per point, we divided total photon count by the number of cycles to estimate photon counts/cycle.

TODE database and GUI

The contents of the TODE database, i.e., individual datasets, were defined in a MATLAB file ("database.mat") stored in the main data folder. This definition file contains a structural array with eleven rows – equivalent to the number of datasets stored in the TODE database – and 18 fields (described in **Supplementary Table 1**) containing metadata and dataset-specific settings for the GUI display. Individual datasets contain raw and processed phosphorescence decay data from Oxyphor 2P phosphorescence lifetime measurements at eleven penetrating arterioles in depths between 0 and 500 μm below the cortical surface. These datasets were generated from primary data stored by the imaging system using custom-written MATLAB scripts as described above and in (Mächler, Fomin-Thunemann et al. 2022). Note that phosphorescence decay profiles and photon counts stored here represent accumulated data after exclusion of individual acquisition cycles potentially contaminated with motion (see above). In addition, the database contains image stacks of every penetrating arteriole visualized with intravascular FITC- or Alexa 680-Dextran as well as low-magnification overviews of the surface vasculature. Image stacks were generated from primary imaging data stored by the imaging system; individual tiff files were combined into a multi-page tiff stack and converted from 16- to 8-bit grayscale to increase performance. Low-magnification overviews were created from maximum intensity projections of image stacks acquired at 4× or 5× magnification, and Adobe Photoshop was used to highlight the artery of interest in the resulting image. The interactive database client GUI was created with the MATLAB App designer (MATLAB 2022a and 2023a; the source code

is available here: https://github.com/NIL-NeuroScience/tode). The TODE GUI was packaged to run either as a MATLAB application or as a standalone application with MATLAB runtime libraries available for different platforms. An export option allows storing the data for each acquired cortical depth of each penetrating arteriole as MATLAB data file for further use.

Organization of TODE Database and GUI

Organization of the experimental data is shown in **Figure 1**. The database stores one directory for each penetrating arteriole containing two subfolders. The ‘pO2’ subfolder stores individual MATLAB files with acquisition parameters, reference images, and results from individual 2P-PLM acquisition runs at 5-6 discrete cortical depths. Reference images are two-photon images acquired at the same depths and show vascular labeling with FITC-Dextran, distribution of the extracellular dye Oxyphor 2P in the tissue, and, optionally, astrocyte labeling with SR101. Further parameters stored in the MATLAB file are spatial coordinates for all points within the acquisition grid, phosphorescence decay curves with corresponding non-linear fit parameters, and estimated pO_2 levels for each point in the grid. A subset of grids is acquired both in square and radial pattern, the latter providing a higher sampling density close to the central arteriole. For a detailed explanation of all variables provided, see **Supplementary Table 2**. The ‘stacks’ subfolder contains high-resolution image stacks recorded after the vasculature has been labeled with dextran-conjugated dyes. In contrast to the reference images within the ‘pO2’ subfolder, the ‘stacks’ subfolder contains image data from the respective penetrating arteriole recorded from the cortical surface down to Layer IV (320-500 µm) or in four cases up to 900 µm at 3-10 µm step size.

For user-friendly access and visualization of the 2P-PLM oxygen imaging data, we created the TODE GUI. The layout of the GUI is shown in **Figure 2**; in the following, we provide a general introduction into the GUI and the functionalities of individual subpanels. A separate window lists the individual dataset, each containing 2P-PLM measurements at several depths around an individual penetrating arteriole. From this panel, loading of the dataset from storage and display of the data in the main panel is initialized. The application only loads the data corresponding to the selected artery and depth allowing for seamless transition between datasets while limiting memory usage. In the main GUI, **Panel a (Metadata)** displays experimental information; it

contains information about animal ID, sex, age in days, and time between surgery and data collection in days. The metadata also provides the artery ID to distinguish datasets when several arteries from the same animal were included. **Panel b (Exposure Overview)** shows the vasculature labeled with fluorescent dextran as a maximum intensity projection of a two-photon image stack acquired with 4× or 5× objective. A red square highlights the penetrating arteriole from which 2P-PLM data was collected. **Panel c (Vasculature Z Stack)** shows two-photon image stacks of the penetrating arteriole labeled with fluorescent dextrans from the cortical surface down to 400-900 µm acquired with a 20× objective. A slider moves through the stack; a switch changes from 1-2× zoom within the imaging plane. **Panel d (Data Display)** displays reference images along with phosphorescence lifetime imaging data. A slider allows brightness adjustment of the currently displayed reference image. The measurement depth can be chosen within the “Depth in µm” block. Here, the user can press the “>>Z plane” button to select the corresponding Z plane in panel c. Once a depth is selected, the user can switch between different reference images in the “Reference Image” block. The “Grid” button in the “Data” block overlays the location of the acquisition grid on top of the reference image; the “Photon Count” button overlays a color-coded grid of photon counts at each data point; the “pO_2” button overlays a colored-coded grid showing pO_2 (in mmHg) at each data point. The switch button underneath the data block with labels “Square” and “Radial” allows the user to show data acquired in radial acquisition grids at selected locations if acquired at this location. The “Clear plot” button clears all plots overlaying the reference image. If some buttons are disabled for individual datasets, the respective data was not acquired. **Panel f (pO_2 Profile Plot)** gives the user the option to draw one or multiple straight lines across the pO_2 landscape shown in Panel e. An interpolated line graph with distance (X, in µm) versus pO_2 value (Y, in mmHg) is created. After selecting the ‘Draw Line’ button, the user draws a line in the reference image of Panel d. Several lines can be drawn by repeatedly choosing the “Draw Line” button. With the “Clear plot” button, the lines in panel d as well as the plots in panel e will be erased. In **Panel f (pO_2 Fit**

Display), an individual data point from the grid in Panel e can be selected after pressing ‘Select point’, and the top graph panel will show the photon count (Y) and the resulting curve from fitting a mono-exponential decay to the data versus time (X, in μs). The bottom graph panel shows the residuals (Y) versus time (X, in μs) for the mono-exponential fit. The ‘Clear plot’ button clears the plots in Panel f.

The “Export MATLAB Matrix” button allows the users to save the 2P-PLM data for the chosen arteriole at the selected depth as MATLAB file. The exported data consists of a structure array for the acquisition run corresponding to the artery at one depth level. The “Export Line Data” button, and the “Export Decay Data” allows the users to save the XY data of the graph.

Benefits of TODE for Oxygen Imaging Dataset Sharing

Over the last decade, increased efforts have been made to standardize curation, storage, and retrieval of experimental data (Policy 2013, Lee and Stvilia 2017, NIH 2020, Siminski, Kim et al. 2021). Public data availability ensures independent validation after publication and facilitates secondary use without need to reperform experimental studies (Ascoli 2015). For less common experimental modalities such as 2P-PLM-based oxygen imaging that lack widely accepted data standards, researchers rely on individual solutions to provide data to other researchers. Therefore, we have developed the TODE database and GUI in MATLAB to simplify access and visualization of 2P-PLM oxygen imaging data generated in our recent study (Mächler, Fomin-Thunemann et al. 2022). Similarly, we recently provided access to 2P-based dynamic vascular imaging data using MATLAB-based solutions (Sridhar, Tian et al. 2014, Uhlirova, Tian et al. 2017).

TODE runs within MATLAB or as a platform-independent stand-alone application which does not require purchasing a MATLAB license. The TODE GUI balances the need for database tools to store and navigate through complex data as well as for tools for efficient data visualization. It enables the customization of data display and data export for use in other applications. MATLAB-based databases are less complex and more relatable to researchers in neuroscience and related fields compared to databases using dedicated database languages such as Structured Query Language (SQL). Given the relative popularity of MATLAB in the field, data can directly be used for further analyses or modeling studies. These could involve computational reconstruction (“graphing”) of the microvascular network (Sakadzic, Roussakis et al. 2010, Gagnon, Sakadzic et al. 2015), applying alternative model assumptions (Saetra, Solbra et al. 2020), or comparison of our in vivo data on oxygen distribution with data from post-mortem structural analyses (Ji, Ferreira et al. 2021). Such modeling studies will contribute to physiologically founded bottom-up models of vascular and hemodynamic changes in response

to changes in neuronal activity to deepen our understanding of cerebral blood flow regulation and non-invasive neuroimaging signals in humans (Gagnon, Sakadzic et al. 2015, Uhlirova, Kilic et al. 2016).

In summary, TODE database and GUI are an example of a tailor-made platform for projects that involve ever-changing data processing streams common in cutting-edge experimental technologies.

Data Availability Statement

The datasets and software for this study can be found on github.

Code Availability Statement

The MATLAB code of the TODE1.0 GUI can be found on github.

Conflict of Interest

The authors declare that the research was conducted in the absence of any commercial or financial relationships that could be construed as a potential conflict of interest.

Acknowledgements

This work was supported by BRAIN R01MH111359 and R01DA050159 grants to AD. LNA acknowledges the support from the Undergraduate Research Opportunities Program (UROP) at Boston University. PM was supported by the Swiss National Science Foundation (P500PB_211149). We thank the Neurovascular Imaging Laboratory at Boston University for software testing and helpful discussion.

References

Ascoli, G. A. (2015). "Sharing Neuron Data: Carrots, Sticks, and Digital Records." PLoS Biol **13**(10): e1002275.

Blinder, P., P. S. Tsai, J. P. Kaufhold, P. M. Knutsen, H. Suhl and D. Kleinfeld (2013). "The cortical angiome: an interconnected vascular network with noncolumnar patterns of blood flow." Nat Neurosci **16**(7): 889-897.

Data Citation Synthesis Group (2014). Joint Declaration of Data Citation Principles. M. M. San Diego CA, FORCE11.

Esipova, T. V., M. J. P. Barrett, E. Erlebach, A. E. Masunov, B. Weber and S. A. Vinogradov (2019). "Oxyphor 2P: A High-Performance Probe for Deep-Tissue Longitudinal Oxygen Imaging." Cell Metab **29**(3): 736-744 e737.

Gagnon, L., S. Sakadzic, F. Lesage, J. J. Musacchia, J. Lefebvre, Q. Fang, M. A. Yucel, K. C. Evans, E. T. Mandeville, J. Cohen-Adad, J. R. Polimeni, M. A. Yaseen, E. H. Lo, D. N. Greve, R. B. Buxton, A. M. Dale, A. Devor and D. A. Boas (2015). "Quantifying the microvascular origin of BOLD-fMRI from first principles with two-photon microscopy and an oxygen-sensitive nanoprobe." J Neurosci **35**(8): 3663-3675.

Gonzalez-Lima, F. and A. Cada (1994). "Cytochrome oxidase activity in the auditory system of the mouse: a qualitative and quantitative histochemical study." Neuroscience **63**(2): 559-578.

Heeger, D. J. and D. Ress (2002). "What does fMRI tell us about neuronal activity?" Nature Reviews Neuroscience **3**(2): 142-151.

Ji, X., T. Ferreira, B. Friedman, R. Liu, H. Liechty, E. Bas, J. Chandrashekar and D. Kleinfeld (2021). "Brain microvasculature has a common topology with local differences in geometry that match metabolic load." Neuron **109**(7): 1168-1187.e1113.

Kim, J., S. Kim, H. M. Cho, J. H. Chang and S. Y. Kim (2020). "Data sharing policies of journals in life, health, and physical sciences indexed in Journal Citation Reports." PeerJ **8**: e9924.

Lecoq, J., A. Parpaleix, E. Roussakis, M. Ducros, Y. Goulam Houssen, S. A. Vinogradov and S. Charpak (2011). "Simultaneous two-photon imaging of oxygen and blood flow in deep cerebral vessels." Nat Med **17**(7): 893-898.

Lee, D. J. and B. Stvilia (2017). "Practices of research data curation in institutional repositories: A qualitative view from repository staff." PLoS One **12**(3): e0173987.

Li, B., R. Ohtomo, M. Thunemann, S. R. Adams, J. Yang, B. Fu, M. A. Yaseen, C. Ran, J. R. Polimeni, D. A. Boas, A. Devor, E. H. Lo, K. Arai and S. Sakadzic (2019). "Two-photon microscopic imaging of capillary red blood cell flux in mouse brain reveals vulnerability of cerebral white matter to hypoperfusion." J Cereb Blood Flow Metab: 271678X19831016.

Mächler, P., N. Fomin-Thunemann, M. Thunemann, M. J. Saetra, M. Desjardins, K. Kilic, L. N. Amra, E. A. Martin, I. A. Chen, I. Sencan-Egilmez, B. Li, P. Saisan, J. X. Jiang, Q. Cheng, K. L.

Weldy, D. A. Boas, R. B. Buxton, G. T. Einevoll, A. M. Dale, S. Sakadzic and A. Devor (2022). "Baseline oxygen consumption decreases with cortical depth." PLoS Biol **20**(10): e3001440.

NIH. (2020). "Final NIH Policy for Data Management and Sharing Notice." from https://grants.nih.gov/grants/guide/notice-files/NOT-OD-21-013.html.

Nosek, B. A., G. Alter, G. C. Banks, D. Borsboom, S. D. Bowman, S. J. Breckler, S. Buck, C. D. Chambers, G. Chin, G. Christensen, M. Contestabile, A. Dafoe, E. Eich, J. Freese, R. Glennerster, D. Goroff, D. P. Green, B. Hesse, M. Humphreys, J. Ishiyama, D. Karlan, A. Kraut, A. Lupia, P. Mabry, T. Madon, N. Malhotra, E. Mayo-Wilson, M. McNutt, E. Miguel, E. L. Paluck, U. Simonsohn, C. Soderberg, B. A. Spellman, J. Turitto, G. VandenBos, S. Vazire, E. J. Wagenmakers, R. Wilson and T. Yarkoni (2015). "Promoting an open research culture." Science **348**(6242): 1422-1425.

NSF. (2021). "Proposal & Award Policies & Procedures Guide." from https://www.nsf.gov/pubs/policydocs/pappg22_1/.

Policy, T. W. H. O. o. S. a. T. (2013). "Expanding public access to the results of federally funded research.", from http://www.whitehouse.gov/blog/2013/02/22/expanding-public-access-results-federally-funded-research.

Roome, C. J. and B. Kuhn (2014). "Chronic cranial window with access port for repeated cellular manipulations, drug application, and electrophysiology." Front Cell Neurosci **8**: 379.

Rubel, O., A. Tritt, R. Ly, B. K. Dichter, S. Ghosh, L. Niu, P. Baker, I. Soltesz, L. Ng, K. Svoboda, L. Frank and K. E. Bouchard (2022). "The Neurodata Without Borders ecosystem for neurophysiological data science." Elife **11**.

Saetra, M. J., A. V. Solbra, A. Devor, S. Sakadzic, A. M. Dale and G. T. Einevoll (2020). "Spatially resolved estimation of metabolic oxygen consumption from optical measurements in cortex." Neurophotonics **7**(3): 035005.

Sakadzic, S., E. Roussakis, M. A. Yaseen, E. T. Mandeville, V. J. Srinivasan, K. Arai, S. Ruvinskaya, A. Devor, E. H. Lo, S. A. Vinogradov and D. A. Boas (2010). "Two-photon high-resolution measurement of partial pressure of oxygen in cerebral vasculature and tissue." Nat Methods **7**(9): 755-759.

Science Magazine. (2023). "Editorial Policies." from https://www.science.org/content/page/science-journals-editorial-policie.

Siminski, S., S. Kim, A. Ahmed, J. Currie, A. Benns, A. Ragsdale, M. Javanbakht, P. M. Gorbach and C. P. C. Investigators (2021). "A Virtual Data Repository Stimulates Data Sharing in a Consortium." Online J Public Health Inform **13**(3): e19.

SpringerNature. (2023). "Research data policy." from https://www.springernature.com/gp/authors/research-data-policy.

Sridhar, V. B., P. Tian, A. M. Dale, A. Devor and P. A. Saisan (2014). "Neurovascular Network Explorer 1.0: a database of 2-photon single-vessel diameter measurements with MATLAB® graphical user interface." Frontiers in Neuroinformatics **8**.

Uhlirova, H., K. Kilic, P. Tian, S. Sakadzic, L. Gagnon, M. Thunemann, M. Desjardins, P. A. Saisan, K. Nizar, M. A. Yaseen, D. J. Hagler, Jr., M. Vandenberghe, S. Djurovic, O. A. Andreassen, G. A. Silva, E. Masliah, D. Kleinfeld, S. Vinogradov, R. B. Buxton, G. T. Einevoll, D. A. Boas, A. M. Dale and A. Devor (2016). "The roadmap for estimation of cell-type-specific neuronal activity from non-invasive measurements." Philos Trans R Soc Lond B Biol Sci **371**(1705).

Uhlirova, H., P. Tian, K. Kılıç, M. Thunemann, V. B. Sridhar, H. Bartsch, A. M. Dale, A. Devor and P. A. Saisan (2017). "Neurovascular Network Explorer 2.0: A Database of 2-Photon Single-Vessel Diameter Measurements from Mouse SI Cortex in Response To Optogenetic Stimulation." Frontiers in Neuroinformatics **11**.

Weber, B., A. L. Keller, J. Reichold and N. K. Logothetis (2008). "The microvascular system of the striate and extrastriate visual cortex of the macaque." Cereb Cortex **18**(10): 2318-2330.

Wilkinson, M. D., M. Dumontier, I. J. Aalbersberg, G. Appleton, M. Axton, A. Baak, N. Blomberg, J.-W. Boiten, L. B. da Silva Santos, P. E. Bourne, J. Bouwman, A. J. Brookes, T. Clark, M. Crosas, I. Dillo, O. Dumon, S. Edmunds, C. T. Evelo, R. Finkers, A. Gonzalez-Beltran, A. J. G. Gray, P. Groth, C. Goble, J. S. Grethe, J. Heringa, P. A. C. 't Hoen, R. Hooft, T. Kuhn, R. Kok, J. Kok, S. J. Lusher, M. E. Martone, A. Mons, A. L. Packer, B. Persson, P. Rocca-Serra, M. Roos, R. van Schaik, S.-A. Sansone, E. Schultes, T. Sengstag, T. Slater, G. Strawn, M. A. Swertz, M. Thompson, J. van der Lei, E. van Mulligen, J. Velterop, A. Waagmeester, P. Wittenburg, K. Wolstencroft, J. Zhao and B. Mons (2016). "The FAIR Guiding Principles for scientific data management and stewardship." Scientific Data **3**(1): 160018.

Figures and Figure Legends

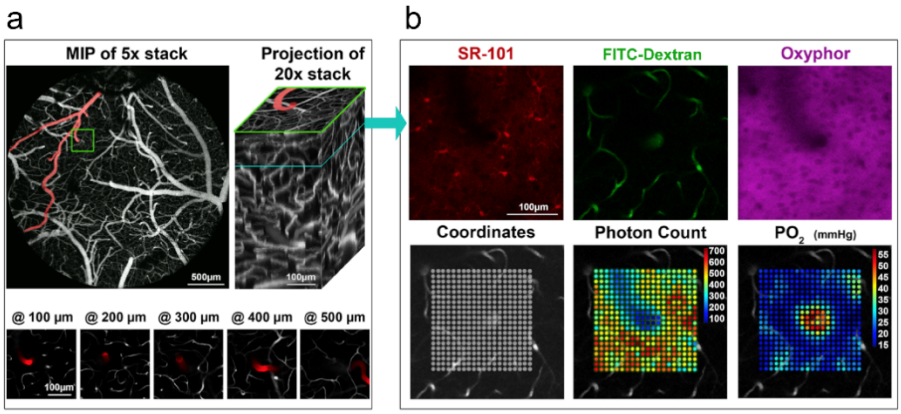

Figure 1. The experimental data stored inside the TODE database is structured based on acquisition strategy. a) One or two diving arterioles per animal were chosen for oxygen imaging. Maximum intensity projections (MIP) of stacks at 4× or 5× magnification show the top view on the vasculature of the exposed cranial cortex including the chosen diving arteriole (green box) branching off a surface artery. Per diving arteriole, Z-stacks at 20× magnification and at additional optical zoom were acquired as illustrated by the Z, XZ, and YZ projections (right) of the Z stack. Individual planes corresponding to the depths where oxygen imaging has been performed are illustrated in the bottom row. b) For each of these depths, Sulforhodamine 101 (SR-101), Fluorescein thiocyanate (FITC)-Dextran, and Oxyphor 2P distribution is included and can be related to the acquired sampling coordinates, their summative photon counts, and their computed oxygen concentration values (pO_2).

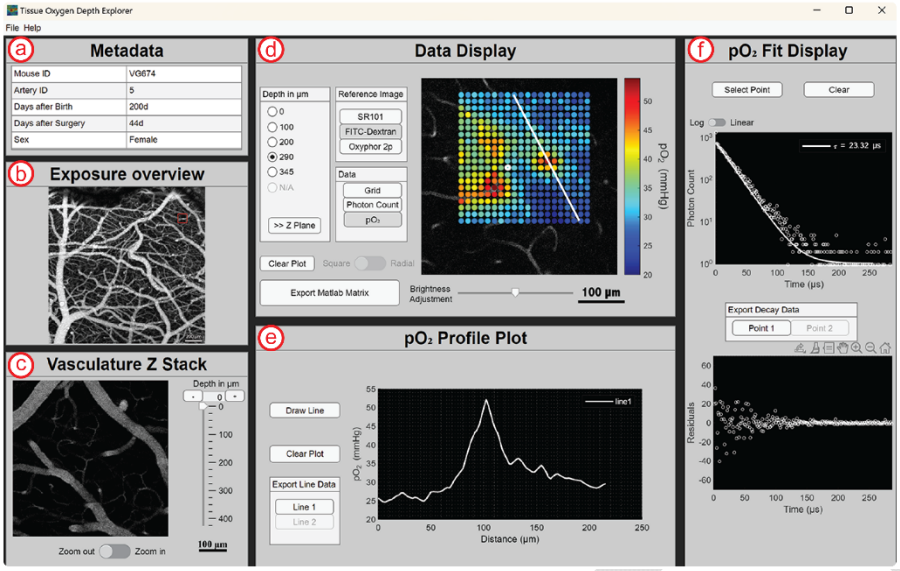

Figure 2. GUI organization and functionality is illustrated on an exemplary selection of the dataset. a) Tabular overview of metadata on experimental animal and arteriole. b) Overview maximum intensity projection of fluorescently labeled vessels. Red square indicates target artery. Shadow on the top left indicates port through which pipette was lowered into the brain to deliver the dye. c) Three-dimensional stack acquired at lower (Zoom out) and higher (Zoom in) magnification. d) Data selection of a single arteriole measured at a depth of 290 µm. The white line represents the user-selected line for which the interpolation profile plot is plotted in panel e. e) The interpolated profile of pO_2 is plotted against distance. f) Top, phosphorescence decay for one point and the corresponding mono-exponential fit of the decay (line) are displayed for one point the user can select in panel e. At the bottom, the residuals of the fit are shown.

Supplementary Information

Supplementary Table 1. Overview of the variables defining the individual datasets stored in the definition file "database.mat". "Low-magnification" and "high-magnification Z stack" refer to Z stacks at 20× magnification and 1× and 2× zoom, respectively. "N" stands for the number of tick labels that vary dependent on the absolute depth of the Z stack.

Variable	*Size*	*Type*	*Unit*	*Description*
ID	1×1	string	[ ]	Dataset identifier
data_depth	1×6	double	[µm]	Depth below cortical surface where datasets were acquired.
data_hasRad	1×6	boolean	[ ]	Dataset with radial acquisition grid available
data_hasSquare	1×6	boolean	[ ]	Dataset with square acquisition grid available
hasFITC	1×1	boolean	[ ]	Dataset contains reference images with vascular staining with FITC-Dextran
hasOxyphor	1×1	boolean	[ ]	Dataset contains reference images with Oxyphor 2P staining
hasSR101	1×1	boolean	[ ]	Dataset contains reference images with Sulforhodamine 101 staining
meta_Artery	1×1	double	[ ]	Artery ID (if more than one artery per animal was acquired)
meta_sex	1×1	char	[ ]	Sex of the animal
Z_depth	2×1	double	[µm]	Maximal depth in Z for low- and high-magnification Z stack
Z_inc	2×1	double	[µm]	Step size in Z for low- and high-magnification Z stack
Z_MajLabels	2×N	cell	[ ]	Major tick labels of Z depth selection slider for low- and high-magnification Z stack
Z_MajTicks	2×N	double	[µm]	Position of major ticks of Z depth selection slider for low- and high-magnification Z stack
Z_MinTicks	2×N	double	[µm]	Position of minor ticks of Z depth selection slider for low- and high-magnification Z stack
Z_Offset	2×1	double	[µm]	Z offset (depth) for low- and high-magnification Z stack
Z_Overview	1×1	double	[ ]	Magnification of overview image
Z_slider	2×2	double	[µm]	Minimal and maximal depth in Z for low- and high-magnification Z stack
Z_Stack	2×1	double	[ ]	Number of planes across along Z for low- and high-magnification Z stack

Supplementary Table 2. Overview of variables provided in the individual datasets of the TODE database. Variables are stored in one data file (.mat) per arteriole and depth; if data from rectangular and circular acquisition grid are available, two individual files are stored. Abbreviations: n_{Points}, number of points where phosphorescence decays were acquired (here: 400); n_{Bins}, number of bins per decay (here: $2^8 = 256$).

Variable name	*Size*	*Type*	*Unit*	*Description*
Main array: pO2				
data	n_{Bins}×n_{Points}	double	[ ]	Photon counts per time bin and point (sum across repetitions and iterations)
dbEntry	1×1	struct		Information on experiment and animal (*see below*)
fitC2	n_{Points}×1	double		Parameter C_2 (i.e., τ from mono-exponential fit)
fitDiag	n_{Points}×1	struct		Diagnostic information on mono-exponential fit (*see below*)
fittedCurve	n_{Points}×1×n	double	[ ]	Fitted mono-exponential decay curve
pO2Value	n_{Points}×1	double	[mmHg]	pO_2 value estimated from τ using Stern-Volmer equation
photonCountCols	n_{Points}×3	double		RGB tuple describing color of individual point in photon count grid
pixelSizeX	1×1	double	[µm]	Pixel size (resolution) of acquired data in X dimension
pixelSizeY	1×1	double	[µm]	Pixel size (resolution) of acquired data in Y dimension
PLIMCyclePeriod	1×1	double	[µs]	Period of single acquisition cycle
PLIMCyclesPerPoint	1×1	double	[ ]	Number of acquisition cycles per point
PLIMExcitationTime	1×1	double	[µs]	Duration of excitation gate
PLIMRepetitions	1×1	double	[ ]	Number of repetitions per acquisition cycle per point
PLIMTimeBin	1×1	double	[µs]	Temporal resolution of decay data
pO2Cols	n_{Points}×3	double		RGB tuple describing color of individual point in pO2 grid
PointsX	1×n_{Points}	double	[ ]	Relative location of Points in × dimension
PointsY	1×n_{Points}	double	[ ]	Relative location of Points in Y dimension
references	1×3	struct		Reference images (*see below*)
sum	n_{Points}×1	double	[ ]	Temporal sum of counted photons per point
tNew	n_{Bins}×1	double	[µs]	Time vector for photon decay data
Sub-array: dbEntry				
date	1×1	string		Date of experiment
mouseID	variable	char		Animal identification (lab-internal)
mouseStrain	variable	char		Animal strain (lab-internal)
mouseDOB	1×1	string		Animal date of birth
mouseSurgery	1×1	string		Date of surgery
artery	1×1	double		Artery identification
Sub-array: references				
info	variable	char		Dye (SR101, FITC, or Oxyphor 2P)
image	512×512	uint8		Image data
Sub-array: fitDiag				
cAll	1×3	double		Solution of the non-linear fit (C_1, C_2, C_3)
resnorm	1×1	double		Squared norm of the residual
resid	n_{Points}×1	double		Residuals
output	1×1	struct		Information about the optimization process (refer to lsqlnonlin for reference)
lambda	2×1	struct		Lagrange multipliers at the solution
jacobinian	n_{Points}×3	double		Jacobian at the solution